科技學刊　第 16 卷 科技類 第 2 期　頁 81-90 中華民國 96 年 5 月

EFFECTS OF NON-NEWTONIAN COUPLE STRESSES ON THE STABILITY OF JOURNAL BEARINGS WITH FINITE LENGTHS

Jaw-Ren Lin, Rong-Fang Lu, Chih-Yi Chang and Won-Hsion Liao

Department of Mechanical Engineering
Nanya Institute of Technology
Taoyuan, Taiwan 32091, R. O. C.

ABSTRACT

On the basis of the Stokes micro-continuum theory, the linear stability boundary of finite journal bearings with a non-Newtonian couple stress fluid is presented. Taking into account the couple stress effects resulting from the base oil blended with various additives, the two-dimensional non-Newtonian couple-stress dynamic Reynolds-type equation is numerically solved by the Preconditioned Conjugate Gradient Method. Application of the linear stability theory to the nonlinear journal-motion equations, the equilibrium solutions and the linear dynamic characteristics are then evaluated. From the results obtained, the non-Newtonian couple stresses signify apparent influences on the linear dynamic characteristics and stability behavior of the finite journal bearing. By replacing the classical Newtonian lubricant with the couple stress fluids, the finite journal bearing with $\lambda = 1$ predicts better stiffness characteristics (S_{XX}, S_{XY}, S_{YX} and S_{YY}) and better damping characteristics (D_{XX}, D_{XY} and D_{YX}) at low or moderate values of the steady eccentricity ratio. On the whole, the effects of non-Newtonian couple stresses on the linear stability boundary are more pronounced for the bearing tending to be short and operating at higher steady eccentricity ratios. The present results provide engineers useful information in bearing designing and applications of journal-bearing systems.

Keywords : journal bearings, finite lengths, couple stress effects, Stokes micro-continuum theory, linear stability characteristics

Ⅰ. INTRODUCTION

The steady-state performance is a basic consideration in bearing designing and selection. However, journal bearings under certain disturbances are prone to an oscillation of whirl instability. This oscillation depends upon the bearing operating conditions. When the rotating speed of the journal increases above the whirl threshold speed, the large orbiting amplitudes may endanger bearing components and result in the journal-bearing contact. Understanding of dynamic characteristics of the journal bearings shows therefore great important. Recently, the increasing use of complex fluids as lubricants has been emphasized owing to the requirement of severe operating conditions for the bearing system. Many experimental researches have shown that the use of complex fluids can improve the lubrication properties of hydrodynamic bearings. The presence of dissolved polymer in the lubricant is found by (Oliver, 1988) to result in load-enhancement and friction-reduction effects in a short journal bearing. A base oil blended various additives is observed by (Spikes, 1994) to stabilize the behavior of lubricants in elasto-hydrodynamic contacts. The use of extreme pressure/anti-wear additives is seen by (Scott and Suntiwattana, 1995) to provide beneficial effects on the

frictional performance and the wear of friction material in a wet friction clutch. Because of the conventional continuum theory failing to describe the flow behavior of these kinds of non-Newtonian complex fluids, a micro-continuum theories taking into account the intrinsic motion of material constituents are developed by (Stokes, 1966). The Stokes micro-continuum theory is the development of classical theory allowing for polar effects such as the presence of non-symmetric tensors, body couples and couple stresses. It is intended to take account for particle-size effects. On the ground of the Stokes micro-continuum theory, the couple stress fluid model has been successfully applied to many researches in engineering applications, such as the peristaltic transport by (Shehawey and Mekheimer, 1994), the rolling elements by (Sinha and Singh, 1981) and (Bujurke and Naduvinami, 1990), the line contacts by (Das, 1997), the squeezing film bearings by (Bujurke and Jayaraman, 1982), and the slider bearings by (Ramanaiah, 1979). Although the steady-state performance of short journal bearings has been analyzed by (Lin, 1997) and the dynamic characteristics of short journal bearings have been presented by (Lin, 2001), the analysis of stability for a finite journal bearing is absent. Since the results of journal bearings with finite length show more practical in engineering application, it motivates us an interest in the further study.

On the basis of the Stokes micro-continuum theory, the stability of finite journal bearings with a non-Newtonian couple stress fluid is investigated in the present paper. To account for the couple stress effects resulting from the base oil blended with various additives, the two-dimensional non-Newtonian dynamic Reynolds-type equation is obtained from the Stokes equations of motion. By applying the linear stability theory to nonlinear equations of the journal motion, the equilibrium solutions, the dynamic characteristics, and the stability boundary are obtained. Comparing with the conventional Newtonian-lubricant case, the effects of couple stresses upon the steady-state attitude angle, the dynamic stiffness and damping coefficients, and the stability threshold speed of finite journal bearings for different lengths are discussed with various steady-state eccentricity ratios.

Ⅱ. ANALYSIS

Figure 1 shows the geometrical configuration of the cross section at the mid-plane $z^* = 0$ for a journal rotor supported on a finite bearing. The journal rotor of radius R is rotating with angular velocity ω^* within the bearing shell. The lubricant in the film region is taken to be an incompressible Stokes couple stress fluid.

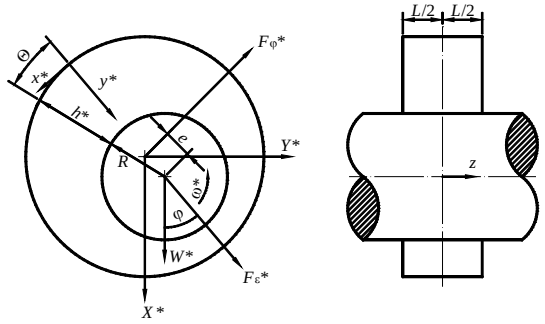

Figure 1 Geometrical configuration of the cross section at the mid-plane $z^* = 0$ for a finite journal bearing.

Under the fundamental assumptions of thin-film lubrication theory, the non-Newtonian couple-stress dynamic Reynolds-type equation can be extended from (Lin, 1997) and (Lin, 2001).

$$\frac{\partial}{R^2\partial\theta}\left\{f^*(h^*,l^*)\frac{\partial p^*}{\partial\theta}\right\}+\frac{\partial}{\partial z^*}\left\{f^*(h^*,l^*)\frac{\partial p^*}{\partial z^*}\right\}$$

$$=6\mu\left\{\left(\omega^*-2\frac{d\varphi}{dt^*}\right)\frac{\partial h^*}{\partial\theta}+2C\frac{d\varepsilon}{dt^*}\cos\theta\right\} \tag{2.1}$$

In the equation $\theta = x^*/R$ is the circumferential coordinate, C is the maximum clearance, φ is the attitude angle, $\varepsilon = e/C$ is the eccentricity ratio, t^* is the time, $h^* = C + e\cos\theta$ is the film thickness, p^* is the film pressure, μ is the shear viscosity, and

$$f^*(h^*,l^*) = h^{*3} - 12l^{*2}h^* + 24l^{*3}\tanh\left(h^*/2l^*\right) \tag{2.2}$$

$$l^* = \left(\eta/\mu\right)^{1/2} \tag{2.3}$$

where η represents the new material constant with the dimension of momentum and is responsible for the couple stress property. As the value of l^* approaches zero,

the non-Newtonian couple-stress dynamic Reynolds-type equation (2.1) reduces to the classical form for the Newtonian-lubricant case by (Gardner, et al., 1985). Introduce the non-dimensional variables and parameters defined as follows.

$$z=\frac{z^*}{L},\quad t=\omega^* t^*,\quad \lambda=\frac{L}{2R},\quad p=\frac{p^* C^2}{\mu\omega^* R^2},\quad h=\frac{h^*}{C},\quad l=\frac{l^*}{C} \tag{2.4}$$

$$f(h,l)=f^*(h^*,l^*)/C^3=h^3-12l^2h+24l^3\tanh\left(h/2l\right) \tag{2.5}$$

where L denotes the length of the bearing, λ is defined as the length-to-diameter ratio, and l the couple stress parameter. As a result, one can obtain the non-Newtonian couple-stress dynamic Reynolds-type equation expressed in a dimensionless form.

$$\frac{\partial}{\partial\theta}\left\{f(h,l)\frac{\partial p}{\partial\theta}\right\}+\frac{1}{4\lambda^2}\frac{\partial}{\partial z}\left\{f(h,l)\frac{\partial p}{\partial z}\right\}$$

$$=6\left\{(1-2\dot{\varphi})(-\varepsilon\sin\theta)+2\dot{\varepsilon}\cos\theta\right\} \tag{2.6}$$

where the dimensionless time derivative $\dot{\varphi}=d\varphi/dt$ and $\dot{\varepsilon}=d\varepsilon/dt$. The boundary conditions for the film pressure are the Reynolds boundary conditions.

$$p=0 \quad \text{at} \quad z=1/2 \quad \text{and} \quad z=-1/2 \tag{2.7}$$

$$p=0 \quad \text{at} \quad \theta=0 \quad \text{and} \quad \theta=\theta_c \tag{2.8}$$

$$\frac{dp}{d\theta}=0 \quad \text{at} \quad \theta=\theta_c \tag{2.9}$$

In the equations it is assumed that the positive pressure terminates at θ_c, the zero pressure-gradient angle. The dimensionless non-Newtonian couple-stress dynamic Reynolds-type equation (2.6) is solved using the preconditioned Conjugate Gradient Method of iteration of (Golub and Van Loan, 1985). The film pressure can be numerically obtained. As a result, the dimensionless hydrodynamic force components can be determined via the integrals.

$$F_\varepsilon=\frac{F_\varepsilon^*}{W^*}=2S\int_0^{1/2}\int_0^{\theta_c} p\cos\theta d\theta dz \tag{2.10}$$

$$F_\varphi=\frac{F_\varphi^*}{W^*}=2S\int_0^{1/2}\int_0^{\theta_c} p\sin\theta d\theta dz \tag{2.11}$$

where W^* denotes the steady load-carrying capacity and S is the Sommerfeld number.

$$S=\frac{\mu\omega^* R}{W^*/L}\left(\frac{R}{C}\right)^2 \tag{2.12}$$

The nonlinear motion equations of the journal rotor in the X^* and Y^* directions are expressed in a dimensionless form respectively.

$$F_X(X,Y,\dot{X},\dot{Y})=F_\varepsilon\cos\varphi-F_\varphi\sin\varphi+1=\omega^2\ddot{X} \tag{2.13}$$

$$F_Y(X,Y,\dot{X},\dot{Y})=F_\varepsilon\sin\varphi-F_\varphi\cos\varphi=\omega^2\ddot{Y} \tag{2.14}$$

In the equations the dimensionless coordinates and angular speed are defined as the follows.

$$X=\varepsilon\cos\varphi,\quad Y=\varepsilon\sin\varphi,\quad \omega=\omega^*\left(mC/W^*\right)^{1/2} \tag{2.15}$$

and m denotes the mass of the journal rotor. The equilibrium solution for the steady state (ε_s,φ_s) is determined from equations (2.13) and (2.14) by letting

$$\varepsilon=\varepsilon_s,\quad \varphi=\varphi_s,\quad \dot{\varepsilon}=0,\quad \dot{\varphi}=0 \tag{2.16}$$

To obtain the dynamic coefficients and the threshold speed of stability, the linear stability theory is applied. Expanding the right hand side of equations (2.13) and (2.14) as a first-order Taylor series about the equilibrium solution, one can obtain the linear motion equations of the journal rotor.

$$\omega^2\Delta\ddot{X}+D_{XX}\Delta\dot{X}+D_{XY}\Delta\dot{Y}+S_{XX}\Delta X+S_{XY}\Delta Y=0 \tag{2.17}$$

$$\omega^2\Delta\ddot{Y}+D_{YX}\Delta\dot{X}+D_{YY}\Delta\dot{Y}+S_{YX}\Delta X+S_{YY}\Delta Y=0 \tag{2.18}$$

where $\Delta X=X-X_s$, $\Delta Y=Y-Y_s$, and the dimensionless stiffness and damping coefficients are defined by the follows.

$$S_{XX}=-\left(\frac{\partial F_X}{\partial X}\right)_s,\quad S_{XY}=-\left(\frac{\partial F_X}{\partial Y}\right)_s,\quad S_{YX}=-\left(\frac{\partial F_Y}{\partial X}\right)_s,$$

$$S_{YY} = -\left(\frac{\partial F_Y}{\partial Y}\right)_s \quad (2.19)$$

$$D_{XX} = -\left(\frac{\partial F_X}{\partial \dot{X}}\right)_s, \quad D_{XY} = -\left(\frac{\partial F_X}{\partial \dot{Y}}\right)_s, \quad D_{YX} = -\left(\frac{\partial F_Y}{\partial \dot{X}}\right)_s,$$

$$D_{YY} = -\left(\frac{\partial F_Y}{\partial \dot{Y}}\right)_s \quad (2.20)$$

Seeking solutions of the linear equations leads to the characteristic equation.

$$\omega^4\lambda_e^4 + \omega^2(D_{XX}+S_{YY})\lambda_e^3 + [\omega^2(S_{XX}+S_{YY}) + D_{XX}D_{YY} - D_{XY}D_{YX}]\lambda_e^2$$

$$+(D_{XX}S_{YY} + D_{YY}S_{XX} - D_{XY}S_{YX} - D_{YX}S_{XY})\lambda_e$$

$$+(S_{XX}S_{YY} - S_{XY}S_{YX}) = 0 \quad (2.21)$$

where λ_e denotes the eigen-value of the system. The threshold speed of linear stability ω_0 can be determined by employing the Routh-Hurwitz stability criterion to this characteristic equation as in (Gardner, et al., 1985).

$$\omega_0 = \left[\frac{\omega_1}{\omega_2 - \omega_3}\right]^{1/2} \quad (2.22)$$

where

$$\omega_1 = D_{XX}D_{YY} - D_{XY}D_{YX} \quad (2.23)$$

$$\omega_2 = \frac{(S_{XX}S_{YY} - S_{XY}S_{YX})(D_{XX}+D_{YY})}{S_{YY}D_{XX} + S_{XX}D_{YY} - S_{YX}D_{XY} - S_{XY}D_{YX}} \quad (2.24)$$

$$\omega_3 = \frac{S_{XX}D_{XX} + S_{YY}D_{YY} + S_{YX}D_{XY} + S_{XY}D_{YX}}{D_{XX}+D_{YY}} \quad (2.25)$$

Ⅲ. RESULTS AND DISCUSSION

Since the dimension of l^* defined in equation (2.3) is of length, it could be identified as the molecular dimension of the couple stress fluid. With the aid of the definition in equation (2.4), the non-Newtonian effects of couple stresses are dominated by the couple stress parameter l. As the value of l approaches zero, the non-dimensional non-Newtonian couple-stress dynamic Reynolds-type equation (2.6) reduces to the classical form of the Newtonian-lubricant case by (Gardner et al., 1985).

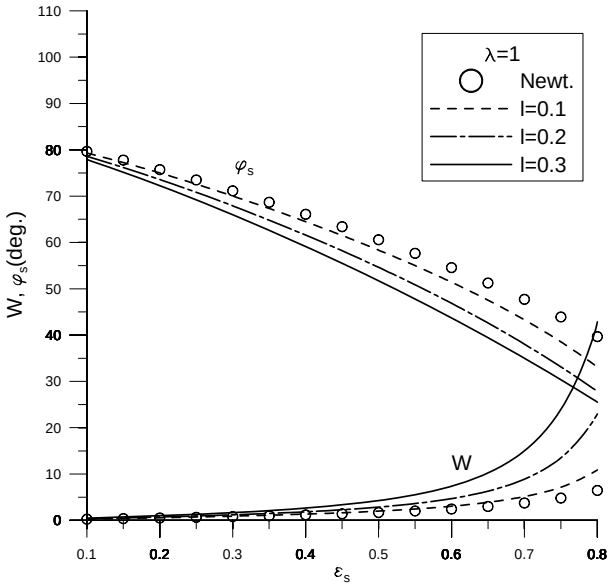

Figure 2 Variation of equilibrium solution φ_s and threshold speed ω_0 with steady eccentricity ratio ε_s for $\lambda = 1$.

Steady performances. Figure 2 presents the variation of steady load-carrying capacity W and the steady attitude angle ψ_s with steady eccentricity ratio ε_s for length-to-diameter ratio $\lambda = 1$. The steady load-carrying capacity W is seen to increase with the steady eccentricity ratio; however, the steady attitude angle ψ_s decreases with the value of ε_s. Comparing with the Newtonian-lubricant case, the bearing with a non-Newtonian couple-stress fluid ($l = 0.1$) results in a higher load capacity and a smaller attitude angle. Increasing the values of l increases the effects of couple stresses on the steady-state performances of the journal bearing.

Linear dynamic coefficients. Figure 3 shows the variation of stiffness coefficient S_{XX} with steady eccentricity ratio ε_s for length-to-diameter ratio $\lambda = 1$. The stiffness coefficient S_{XX} is observed to increase with the steady eccentricity ratio. The effects of couple stress ($l = 0.1$) increase the stiffness S_{XX} especially at higher ε_s as compared to the Newtonian-lubricant case. Increasing the values of couple stress parameter ($l = 0.2$ and $l = 0.3$) increases the effects of couple stresses on the dynamic stiffness coefficient S_{XX}. Figure 4 depicts the variation of stiffness coefficient S_{XY} with

steady eccentricity ratio ε_s for $\lambda=1$. The stiffness coefficient S_{XY} decreases to a minimum and thereafter increases with ε_s. The effects of couple stresses on S_{XY} are seen to be slight at lower ε_s. However, the couple stress effects on the damping coefficient are apparently observed for the bearing operating at higher ε_s.

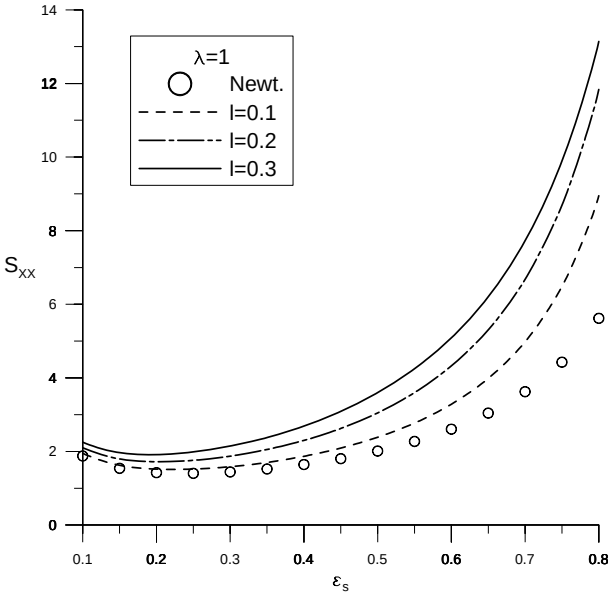

Figure 3　Variation of stiffness coefficient S_{XX} with steady eccentricity ratio ε_s for $\lambda=1$.

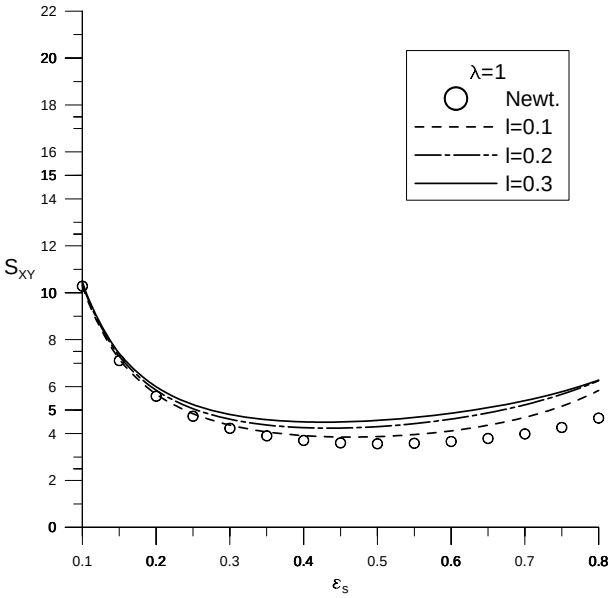

Figure 4　Variation of stiffness coefficient S_{XY} with steady eccentricity ratio ε_s for $\lambda=1$.

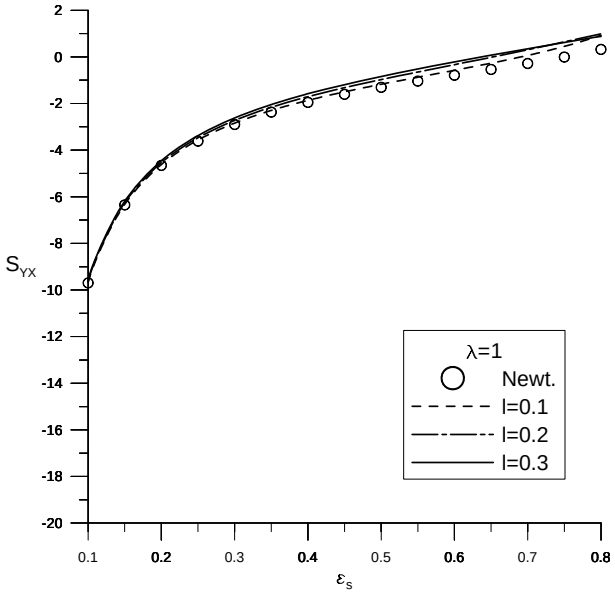

Figure 5　Variation of stiffness coefficient S_{YX} with steady eccentricity ratio ε_s for $\lambda=1$.

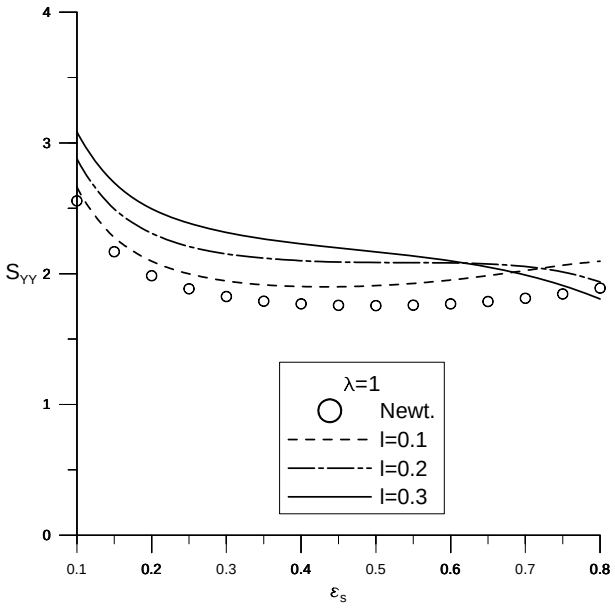

Figure 6　Variation of stiffness coefficient S_{YY} with steady eccentricity ratio ε_s for $\lambda=1$.

Figure 5 shows the variation of stiffness coefficient S_{YX} with steady eccentricity ratio ε_s for $\lambda=1$. It is seen that the stiffness S_{YX} increases rapidly at lower ε_s. Comparing with the classical Newtonian-lubricant case, the effects of couple stress ($l=0.1$, $l=0.2$ and $l=0.3$) increase slightly the stiffness S_{YX} at higher steady eccentricity ratios. Figure 6 presents the variation

of stiffness coefficient S_{YY} with steady eccentricity ratio ε_s for $\lambda = 1$. The effects of couple stresses ($l = 0.1$) are found to provide a higher stiffness coefficient S_{YY} as compared to the classical Newtonian-lubricant case. Increasing the values of couple stress parameter ($l = 0.2$ and $l = 0.3$) enhances the effects of couple stresses on the stiffness S_{YY} at low values of ε_s. However, an interesting event is observed that the effects of couple stresses ($l = 0.3$) resulting in a lower S_{YY} for the bearing operating at higher ε_s as compared to the classical Newtonian-lubricant case. Figure 7 shows the variation of damping coefficient D_{XX} with steady eccentricity ratio ε_s for $\lambda = 1$. The damping coefficient D_{XX} is observed to fall rapidly at lower values of ε_s. Comparing with the classical Newtonian-lubricant case, the effects of couple stresses ($l = 0.1$) give a visible increment in the value of D_{XX} at higher steady eccentricity ratios. Increasing the values of couple stress parameter ($l = 0.2$ and $l = 0.3$) increases the effects of couple stresses on the damping coefficient D_{XX}. Figures 8 and 9 present the variations of damping coefficients D_{XY} and D_{YX} with steady eccentricity ratio ε_s for $\lambda = 1$. The damping coefficients D_{XY} and D_{YX} are observed to decrease rapidly at lower values of the steady eccentricity ratio. Comparing with the classical Newtonian-lubricant case, the effects of couple stresses ($l = 0.1$) increase the value of damping coefficients D_{XY} and D_{YX}. Increasing the values of couple stress parameter ($l = 0.2$ and $l = 0.3$) increases the effects of couple stresses on the damping coefficients at low eccentricity ratios; however, the effects of couple stresses on the value of D_{XY} and D_{YX} are slight for the bearing operating at higher values of the eccentricity ratio near $\varepsilon_s = 0.8$. Figure 10 depicts the variation of damping coefficient D_{YY} with steady eccentricity ratio ε_s for $\lambda = 1$. The value of D_{YY} is observed to decrease with the steady eccentricity ratio. It is found that the effects of couple stresses on the damping coefficient D_{YY} are observed to be slight as compared to the classical Newtonian-lubricant case.

Linear stability threshold speed. The linear stability threshold speed ω_0 is a function of the steady-state eccentricity ratio ε_s. When the values of ω_0 corresponding to ε_s are obtained, the linear stability boundary is determined. Below the value of ω_0 all four eigen-values of λ_e have negative real parts, the steady equilibrium positions for the journal rotor under small disturbances are stable. At the value of ω_0 two ei gen-values locate at the imaginary axis of the complex plane and the journal rotor is neutrally stable. Above the

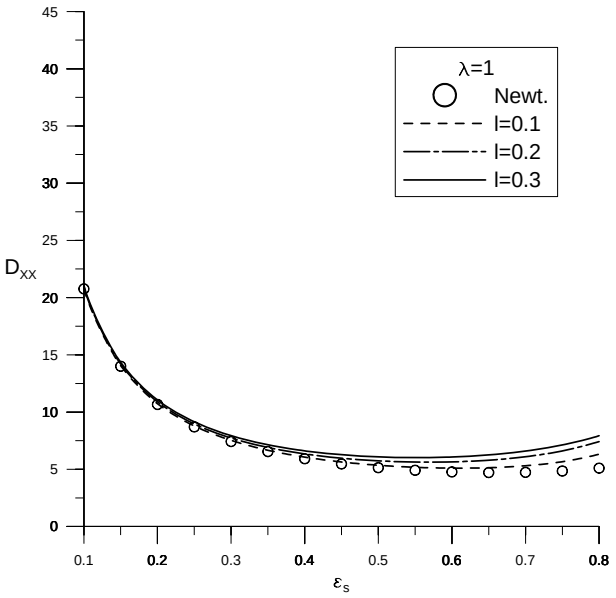

Figure 7 Variation of damping coefficient D_{XX} with steady eccentricity ratio ε_s for $\lambda = 1$.

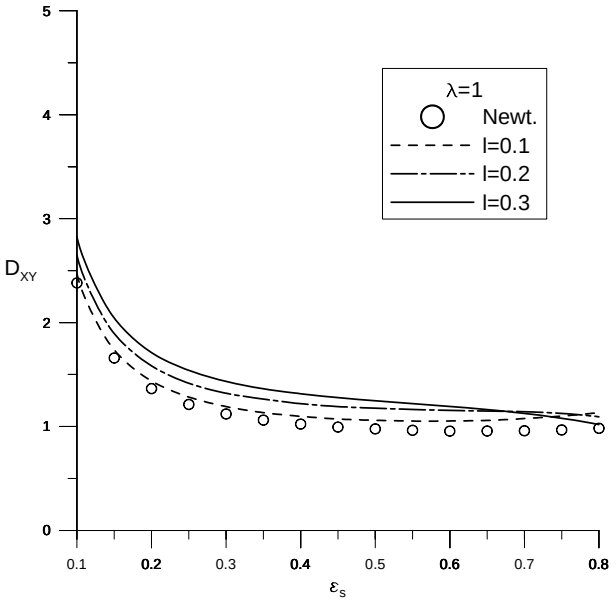

Figure 8 Variation of damping coefficient D_{XY} with steady eccentricity ratio ε_s for $\lambda = 1$.

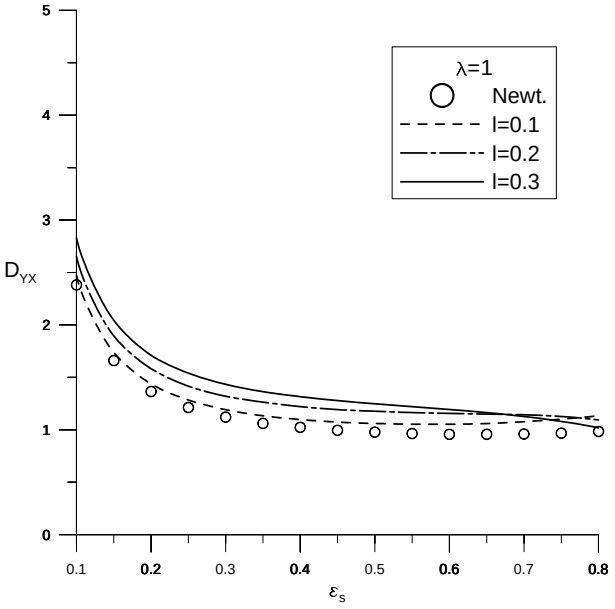

Figure 9　Variation of damping coefficient D_{YX} with steady eccentricity ratio ε_s for $\lambda = 1$.

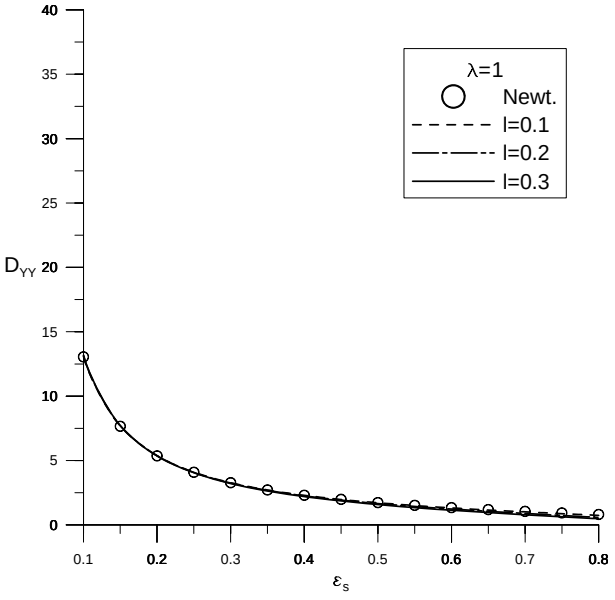

Figure 10　Variation of damping coefficient D_{YY} with steady eccentricity ratio ε_s for $\lambda = 1$.

value of ω_0 two eigen-values cross the imaginary axis into the right half of the complex plane, and the instability sets in for the system. From equation (22) the interactive effects of eight dynamic stiffness and damping coefficients result in the stability threshold speed of the system. Figure 11 shows the variation of stability threshold speed ω_0 with couple stress parameter l at ε_s for $\lambda = 1$. For the bearing operating at low or moderate values of the steady eccentricity ratio ($\varepsilon_s = 0.1$, $\varepsilon_s = 0.2$, $\varepsilon_s = 0.3$, $\varepsilon_s = 0.4$, $\varepsilon_s = 0.5$ and $\varepsilon_s = 0.6$), the threshold speed ω_0 is observed to increase gradually with the value of couple stress parameter. As ε_s increases up to $\varepsilon_s = 0.7$, the stability threshold speed increases rapidly with the couple stress parameter until a maximum, and thereafter decreases rapidly with the value of l. However, when the bearing operating at a higher eccentricity ratio ($\varepsilon_s = 0.8$), the threshold speed ω_0 is found to decrease with l; in addition the decrement is more emphasized at lower values of the couple stress parameter. Since the couple stress parameter is defined by $l = l^*/C = (\eta/\mu)^{1/2}/C$, a material constant η such that $l = 0.2$ or $l = 0.3$ may change the non-Newtonian effects upon the dynamic coefficients S_{YY}, D_{XY} and D_{YX} (shown in Figures 6, 8 and 9) for the bearing operating at higher eccentricity ratio. As a results, the tendency of the variation of stability threshold speed ω_0 with ε_s may vary especially for the bearing with higher values of the couple stress parameter and the eccentricity ratio as shown in Figure 11.

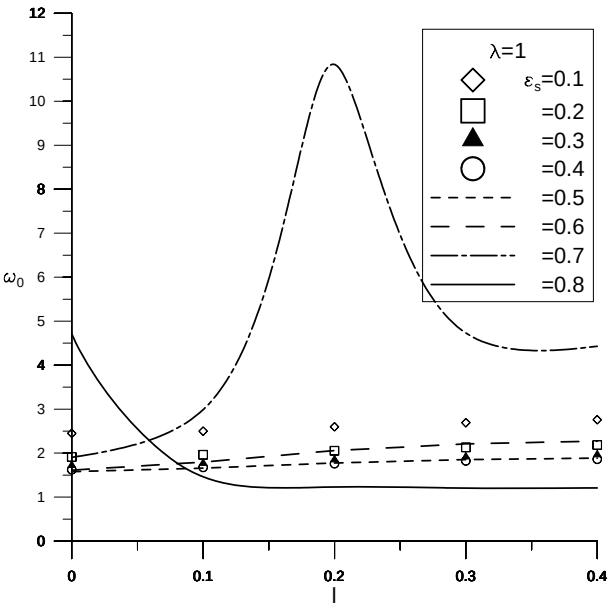

Figure 11　Variation of stability threshold speed ω_0 with couple stress parameter l^* at different steady eccentricity ratios.

Figure 12 presents the variation of stability threshold speed ω_0 with ε_s for $\lambda = 1$. The threshold speed for the classical Newtonian-lubricant case is seen to de

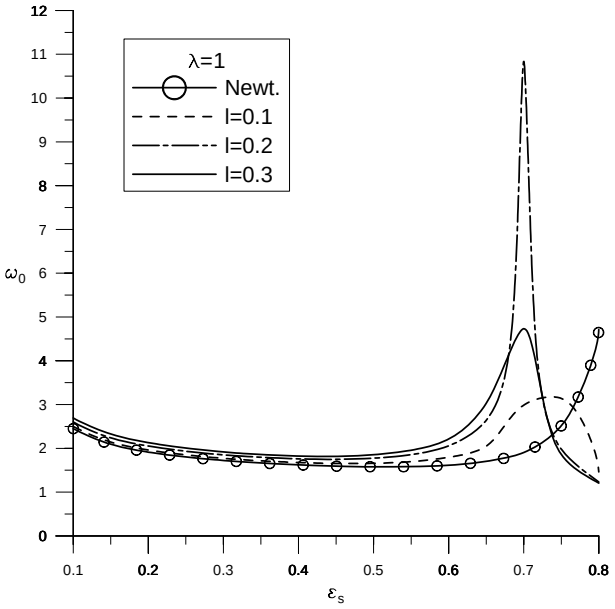

Figure 12 Variation of stability threshold speed ω_0 with steady eccentricity ratio ε_s for $\lambda = 1$.

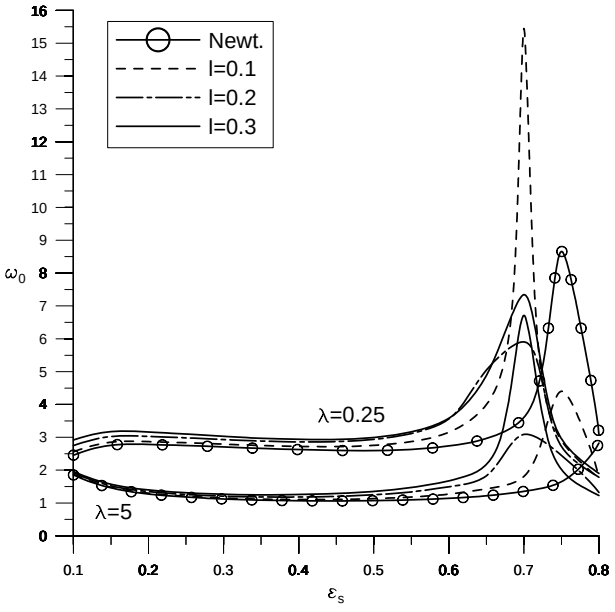

Figure 13 Variation of stability threshold speed ω_0 with steady eccentricity ratio ε_s for different λ.

crease slightly with ε_s until a minimum at is reached, and thereafter rises as ε_s continues to increase. For the bearing lubricated with a couple stress fluid ($l = 0.1$), a maximum threshold speed at $\varepsilon_s = 0.8$ is observed. Increasing the values of l ($l = 0.2$ and $l = 0.3$) shifts the position of the maximum threshold speed to $\varepsilon_s = 0.8$. Comparing with the Newtonian-lubricant case, the effects of couple stresses ($l = 0.1$) yields a higher threshold speed at eccentricity ratios about $\varepsilon_s = 0.76$. Increasing the couple stress parameter ($l = 0.2$) increases the maximum threshold speed up to the value of $\omega_0 = 10.83$ occurring at $\varepsilon_s = 0.7$. However, a maximum threshold speed of $\omega_0 = 4.73$ occurring at $\varepsilon_s = 0.7$ is obtained for the bearing with the couple stress parameter $l = 0.3$. To get a further insight into the effects of bearing length, Figure 13 presents the variation of stability threshold speed ω_0 with the steady eccentricity ratio ε_s for different length-to-diameter ratios ($\lambda = 0.25$ and $\lambda = 5$). It is shown that increasing the bearing length decreases the stability threshold speed. The bearing lubricated with couple stress fluids provides higher stability threshold speeds at low or moderate values of the steady eccentricity ratio depending upon the value of couple stress parameters. The non-Newtonian effects of couple stresses upon the linear stability boundary are more pronounced for the bearing tending to be short and operating at higher eccentricity ratios.

Ⅳ. CONCLUSIONS

Based upon the Stokes micro-continuum theory, the linear stability analysis of finite journal bearings lubricated with a non-Newtonian couple stress fluid is presented. By applying the linear stability theory to the nonlinear journal-motion equations, the linear dynamic characteristics are predicted. According to the results discussed, conclusions are drawn as the following.

The influences of non-Newtonian couple stresses on the dynamic characteristics of the journal-bearing system are significantly apparently. By replacing the classical Newtonian lubricant with the couple stress fluids, the finite journal bearing with $\lambda = 1$ predicts better stiffness characteristics (S_{XX}, S_{XY}, S_{YX} and S_{YY}) and better damping characteristics (D_{XX}, D_{XY} and D_{YX}) at low or moderate values of the steady eccentricity ratio. Comparing with the classical Newtonian-lubricant case, the non-Newtonian couple stress effects provide higher stability threshold speeds at low or moderate eccentric-

ity ratio depending upon the couple stress parameters. Totally the effects of non-Newtonian couple stresses upon the linear stability boundary are more pronounced for the bearing tending to be short and operating at higher steady eccentricity ratios.

ACKNOWLEDGEMENTS

The authors would like to thank the National Science Council of ROC for the support through Grant: NSC-93-2212-E-253-001–.

REFERENCES

Bujurke, N. M. and Jayaraman, G., 1982, The influence of couple stresses in squeeze films, Int. J. Mech. Sci., Vol. 24, pp. 369-976.

Bujurke, N. M. and Naduvinami, N. G., 1990, The lubrication of lightly cylinders in combined rolling, sliding and normal motion with couple stress fluid, Int. J. Mech. Sci., Vol. 32, pp. 969-979.

Das, N. D., 1997, Elastohydrodynamic lubrication theory of line contact: couple stresses fluid model, STLE Trib. Trans., Vol. 40, pp. 353-359.

Gardner, M., Myers, C. J., Savage, M. and Taylor, C., 1985, Analysis of limit cycle response in fluid-film journal bearings using the method of multiple scales, Quart. J. Mech. Appl. Math., Vol. 38, pp. 27-45.

Golub, G. H. and Van Loan, C. F., 1985, Matrix Computation, The John Hopkins University Press, Baltimore, MD.

Lin, J. R., 1997, Static characteristics of rotor bearing system lubricated with couple stress fluids, Computers and Structures, Vol. 62, pp. 175-184.

Lin, J. R., 2001, Linear stability analysis of rotor bearing system: couple stress fluid model, Computers and Structures, Vol. 79, pp. 801-809.

Oliver, D. R., 1988, Load enhancement effects due to polymer thickening in a short model journal bearing, J. Non-Newtonian Fluid Mechanics, Vol. 30, pp. 185-189.

Ramanaiah, G., 1979, Slider bearings lubricated by fluids with couple stress, Wear, Vol. 52, pp. 27-36.

Scott, W. and Suntiwattana, P., 1995, Effect of oil additives on the performance of a wet friction clutch material, Wear, Vol. 181-183, pp. 850-855.

Shehawey, E. F. E. and Mekheimer, K. S., 1994, Couple stresses in peristaltic transport of fluids, J. Phys. D: Appl. Phys, Vol. 27, pp. 1163-1170.

Sinha, P. and Singh, C., 1981, Couple stresses in the lubrication of rolling contact bearings considering cavitation, Wear, Vol. 67, pp. 85-91.

Spikes, A. H., 1994, The behavior of lubricants in contacts: current understanding and feature possibilities, J. Proc. Instn. Mech. Engrs., Vol. 28, pp. 3-15.

Stokes, V. K., 1966, Couple stresses in fluids, Phys. Fluids, Vol. 9, pp. 1709-1715.

Received 24 April 2007
Accepted 21 June 2007

Journal of Science and Technology Vol.16, Science and Technology, No.2, pp. 81-90 May 2007

非牛頓偶應力效應對於有限長頸軸承穩定性能之影響

林昭仁　盧榮芳　張志毅　廖文賢

南亞技術學院機械工程系

摘　　要

在史托克微連體理論基礎下，本文主要是在探討有限長頸軸承採用非牛頓偶應力流體爲潤滑劑時之線性穩定性能。爲能考慮一般機油在加入各種添加劑後所產生之非牛頓偶應力效應，本文利用二維非牛頓偶應力動態型雷諾方程式以求出有限長頸軸承之液動油膜壓力與力量。接著應用線性穩定理論，求得有限長頸軸承之動態剛度與阻尼係數，進而分析系統之穩定性能。根據所得結果，在低與中偏心比情況下，非牛頓偶應力效應有助於有限長（$\lambda=1$）頸軸承之剛度係數（S_{XX}，S_{XY}，S_{YX} 與 S_{YY}）與阻尼係數（D_{XX}，D_{XY} 與 D_{YX}）之提升。整體而言，非牛頓偶應力效應對於頸軸承之線性穩定門檻速率之影響在長徑比愈小且偏心比愈高時，更爲顯著。本文之研究結果，可提供工程師與業界在設計與應用頸軸承系統時一個有用之參考依據。

關鍵詞：頸軸承、有限長度、偶應力效應、微連體理論、線性穩定性能